

(AGN)²

7. Interstellar Dust

Week 9
April 29 (Monday), 2024

updated on 04/26, 15:52

선광일 (Kwangil Seon)
KASI / UST

7.1 Introduction

- H II regions and PNe contain dust particles in addition to the gas.
 - The effects of this dust on the properties of the nebulae are by no means negligible.
 - Contents
 - ▶ Evidence for the existence of dust in nebulae
 - ▶ Its effects on physical conditions within the gas and the observational data
 - ▶ How the measurements can be corrected for these effects.
 - ▶ Measurements of the radiation of both H II regions and PNe
 - ▶ Dynamical effects that result from the dust

7.2 Interstellar Extinction

- Extinction = Absorption + Scattering
 - It results in the reduction in the amount of light in a line of sight, if radiation from other sightlines is not scattered into the line of sight.

$$I_\lambda = I_{\lambda 0} \exp(-\tau_\lambda)$$

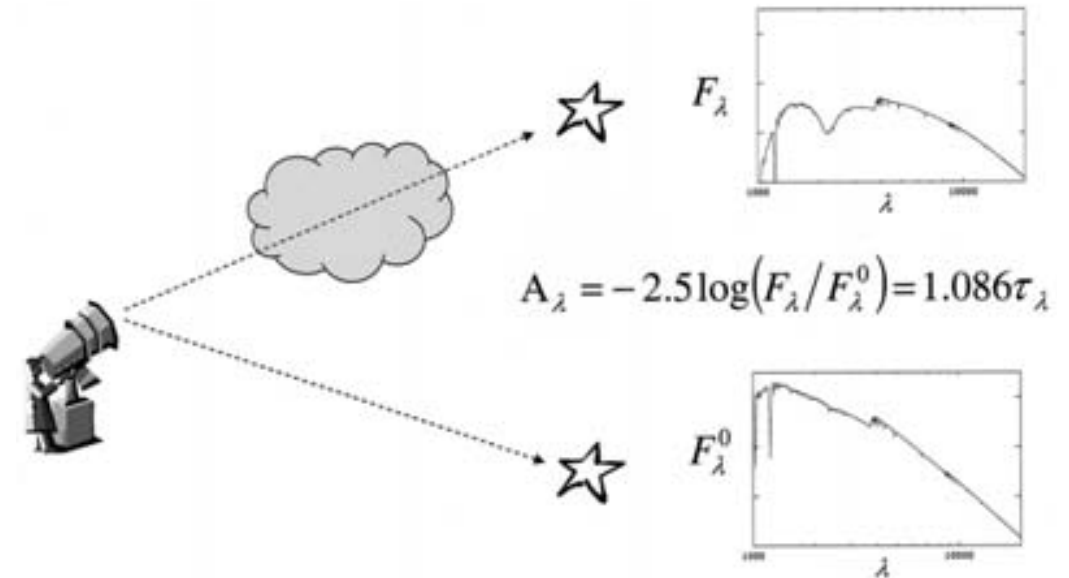
where $I_{\lambda 0}$ is the intensity that would be received at the earth in the absence of interstellar extinction along the line of sight. I_λ is the intensity actually observed, and τ_λ is the optical depth.

- This equation applies to stars, in which we observe the total flux F_λ .
- The interstellar extinction is specified by the values of τ_λ along the ray to the star or nebula in question.
- Extinction in the optical region is largely due to scattering. Nevertheless, the process is very often referred to as interstellar absorption.

- Pair Method
 - The interstellar extinction is derived by spectrophotometric measurements of pairs of stars that have identical spectral types.
 - The ratio of their fluxes depends on the ratio of their distances and on the difference in the optical depths along the two lines of sight.

$$\frac{F_\lambda(1)}{F_\lambda(2)} = \frac{F_{\lambda 0}(1)e^{-\tau_\lambda(1)}}{F_{\lambda 0}(2)e^{-\tau_\lambda(2)}} = \left(\frac{D_2}{D_1}\right)^2 e^{-[\tau_\lambda(1) - \tau_\lambda(2)]}$$

$$\tau_\lambda(1) - \tau_\lambda(2) \approx \tau_\lambda(1)$$



[Fitzpatrick] Astrophysics of Dust, p35

- By comparing a slightly reddened or nonreddened star with a reddened star, it is possible to determine $\tau_\lambda(1) - \tau_\lambda(2) \approx \tau_\lambda(1)$, which represents the interstellar extinction along the path to the more reddened star.
- The ratio of distances may be determined (1) by making measurements at sufficiently long wavelengths because $\tau_\lambda \rightarrow 0$ as $\lambda \rightarrow \infty$ and (2) by the parallax measurements.

- Extinction curves (extinction laws, reddening laws)

- The wavelength dependence of the extinction along most lines of sight through the diffuse ISM are similar enough for it to be expressed as a reddening law:

$$\tau_\lambda = Cf(\lambda)$$

where C depends on the star, but $f(\lambda)$ is approximately the same for most stars in the Galaxy.

This implies that the optical properties of the dusts are similar in the ISM.

- The functional shape of $f(\lambda)$ may be determined by the flux ratio between two different wavelengths (λ_1 and λ_2):

$$\frac{F_{\lambda_1}}{F_{\lambda_2}} = 10^{-c[f(\lambda_1) - f(\lambda_2)]} \text{ where } c = 0.434C, \text{ or } \frac{F_{\lambda_1}}{F_{\lambda_2}} = 10^{-\left(A_{\lambda_1} - A_{\lambda_2}\right)/2.5}$$

$$\Leftrightarrow \frac{F_\lambda}{F_{\lambda 0}} = 10^{-A_\lambda/2.5} = e^{-\tau_\lambda} \text{ and } A_\lambda = -2.5 \log_{10}(F_\lambda/F_{\lambda 0}) = 1.086\tau_\lambda$$

where A_λ is the **total extinction** in magnitudes at λ .

- This ideal leads to define the selective extinction:

selective extinction: the difference in the extinction between two wavelengths = $A_{\lambda 1} - A_{\lambda 2}$

color excess: $E(B - V) = A_B - A_V$ = selective extinction between the B and V filters ($\sim 4400\text{\AA}$ and 5500\AA , respectively)

$E(B - V)$ depends on the grain properties (size and composition) and the column density of material along the line of sight.

- The **ratio of total to selective extinction** $R_V = A_V/E(B - V)$ compares the (“absolute”) extinction and (“relative”) reddening properties of grains.

This value would be sensitive only to the grain properties (composition, size, and shape).

$R_V \approx 3.1$ is typical in the diffuse ISM.

$R_V \approx 5.5$ along the line of sight to the Orion Nebula.

- The **extinction per unit column density of hydrogen**, $A_V/N(\text{H})$, depends on grain properties, but also on the dust-to-gas ratio. Typical values are $A_V/N(\text{H}) \approx 5.31 \times 10^{-22} \text{ mag cm}^2$.
- Note that the functional shape of $f(\lambda)$ would be better represented by the ratio of $f(\lambda)$, rather than the flux ratio, between two different wavelengths. For instance, A_λ/A_V .

Or it can be represented by a ratio of $E(\lambda - V)$ to $E(B - V)$.

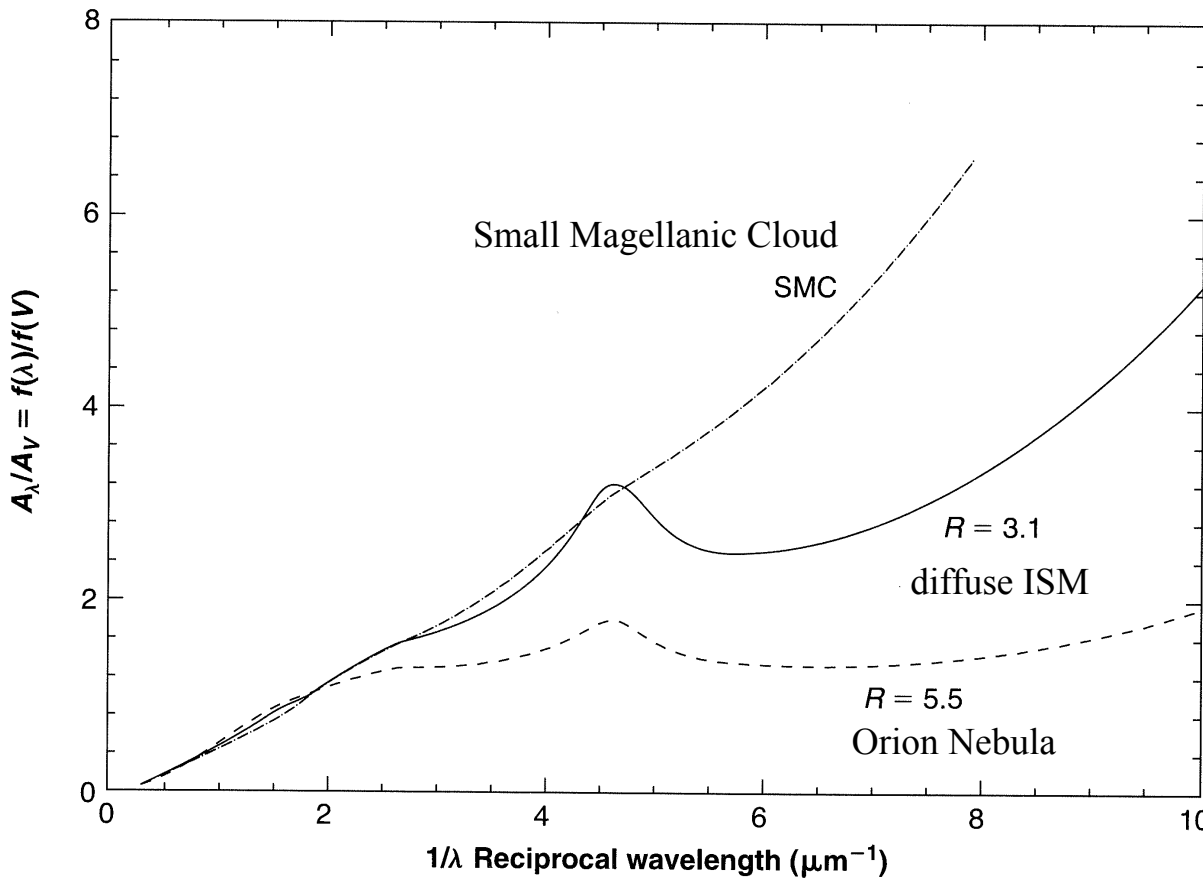


[Figure 7.1]

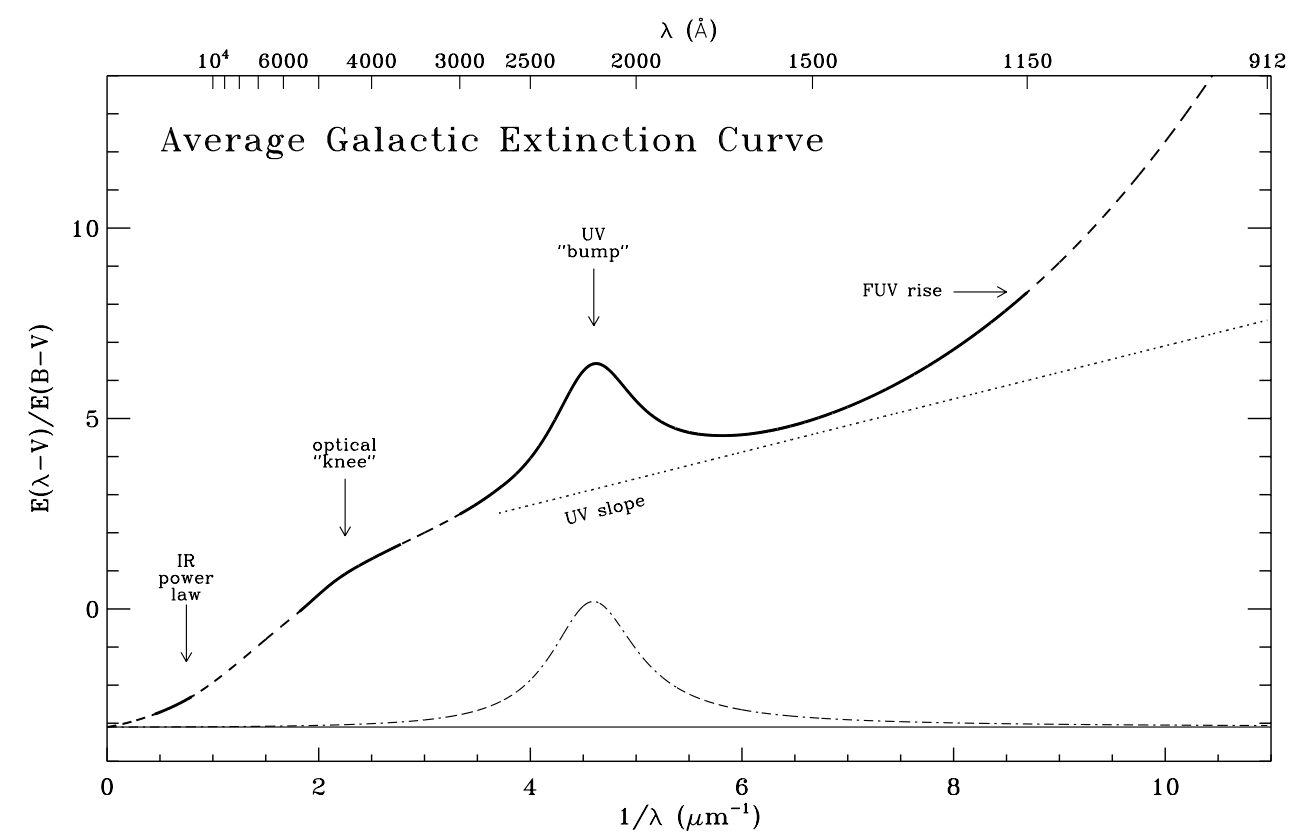


[Figure 2, Fitzpatrick]

-
- The detailed forms are sensitive to both the grain composition and their size.
 - Compositions
 - ▶ The broad bump centered near $4.6 \mu\text{m}^{-1}$ or 2175\AA is thought to be due to PAHs (or other particles rich in carbon, hydrogenated amorphous carbon, etc.)
 - ▶ May small features occur in the IR and indicates that silicate-rich compounds and ices must be present.
 - ▶ The differences in the overall extinction curves show that at least two or more are responsible for the extinction: graphite + “astronomical silicate” (such as olivine $(\text{Mg}, \text{Fe})_2 \text{SiO}_4$).
 - Grain sizes
 - ▶ The form of the curves is affected by the grain sizes.
 $A_\lambda \approx \text{constant}$ for $\lambda \ll a$ (gray extinction - the same at all wavelengths)
 $A_\lambda \propto \lambda^{-4}$ for $\lambda \gg a$ (Rayleigh scattering limit)
 - ▶ The fact that $A_\lambda \propto \lambda^{-1}$ implies that a wide range of grain sizes must be present.
 - ▶ Regions like Orion, with a large R_V (flat curve), have a grain size distribution that is weighted to larger than average sizes, or perhaps deficient in smaller grains.
 - ▶ The SMC extinction may be due to a preponderance of very small particles (steeply rising).

-
- Extinction Correction
 - The observed line ratio at two emission lines would be related to the original line ratio:

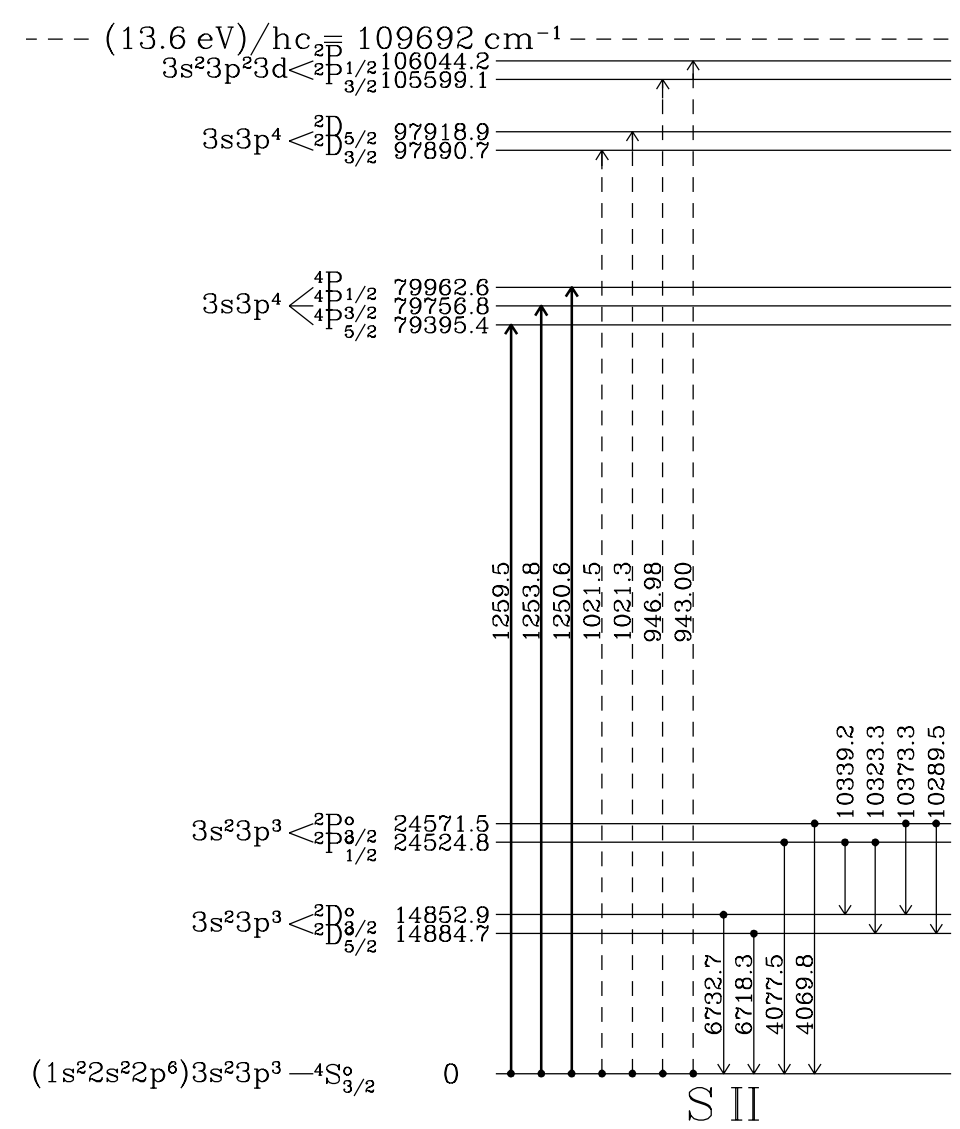
$$\frac{I_{\lambda_1}}{I_{\lambda_2}} = \frac{I_{\lambda_1 0}}{I_{\lambda_2 0}} e^{-(\tau_{\lambda_1} - \tau_{\lambda_2})} = \frac{I_{\lambda_1 0}}{I_{\lambda_2 0}} e^{-(\sigma_{\lambda_1} - \sigma_{\lambda_2})nl}$$

where σ_λ = the extinction cross section at λ , n = the number density, and l = the pathlength

The correction term depends on the shape of the extinction curve ($\sigma_\lambda = \sigma_V(A_\lambda/A_V)$) and on the amount of extinction (column density = nl).

- To find the amount of correction, the principle is (1) to assume an appropriate reddening curve, for instance, that with $R_V = 3.1$, and (2) to use two emission lines for which the relative intensities are well known independently.

- Ideal line ratio
 - The ideal line ratio to determine the amount of extinction is one that is completely independent of physical conditions and that is easy to measure in all nebulae.
 - The best lines would be a pair with the same upper level, whose intensity ratio would depend only on the ratio of their transition probabilities.
- Examples:
 - An example that is close to the ideal is to use the [S II] lines:
 - ▶ [S II] $^4S - ^2P$ $\lambda\lambda 4069, 4076$ and
 - ▶ [S II] $^2D - ^2P$ $\lambda\lambda 10287, 10320, 10336, 10370$
 - ▶ Both multiplets arise from a doublet upper term, and the relative populations in the two levels depend slightly on electron density.
 - ▶ This [S II] ratio has been used in a few galaxies. However, they are very weak in PNe and SNRs.
 - ▶ Contamination due to infrared OH atmospheric emission.
 - A somewhat easier observational method:
 - ▶ compare an H I Paschen line with a Balmer line
 - ▶ $P\delta \lambda 10049$ and $H\epsilon \lambda 3970$
 - ▶ Both arise from the excited terms with $n = 7$. The relative strengths depend slightly on the temperature.
 - ▶ However, their variation in the ratio is quite small over a wide range of temperature.
 - ▶ Contamination by IR night-sky emission + insensitivity of CCDs.
 - He II $\lambda 4686/\lambda 1640$ ratio



- The most frequently used method: **Balmer Decrement**
 - Ratios of two or more H I Balmer lines - for instance, $H\alpha/H\beta$ and $H\beta/H\gamma$
 - The upper levels are not the same for the two lines. However, the line ratios are relatively insensitive to temperature.
 - The Balmer lines are strong and occur in the part of the spectrum that are usually observed.
 - The different pairs of Balmer lines give the same result, confirming observationally the recombination theory.
 - Nebulae are observed to differ greatly in the amount of extinction.

$$\frac{F_{H\alpha}}{F_{H\beta}} = \frac{h\nu_{H\alpha}}{h\nu_{H\beta}} \frac{\alpha_{\text{eff},H\alpha}}{\alpha_{\text{eff},H\beta}} = 2.860 T_4^{-0.068+0.027 \ln T_4}$$

$$\alpha_{\text{eff},H\alpha} \approx 1.17 \times 10^{-13} T_4^{-0.942-0.031 \ln T_4} \text{ cm}^3 \text{ s}^{-1}$$

$$\alpha_{\text{eff},H\beta} \approx 3.03 \times 10^{-14} T_4^{-0.874-0.058 \ln T_4} \text{ cm}^3 \text{ s}^{-1}$$

The table and formula for the recombination rate coefficients are from Chapter 14 of the Draine's textbook.

Table 14.2 Case B Hydrogen Recombination Spectrum^a for $n_e = 10^3 \text{ cm}^{-3}$

	5000	10,000	20,000
$\alpha_B (\text{cm}^3 \text{s}^{-1})$	4.53×10^{-13}	2.59×10^{-13}	1.43×10^{-13}
$\alpha_{\text{eff},2s}/\alpha_B$	0.305	0.325	0.356
$\alpha_{\text{eff},H\alpha} (\text{cm}^3 \text{s}^{-1})$	2.20×10^{-13}	1.17×10^{-13}	5.96×10^{-14}
$\alpha_{\text{eff},H\beta} (\text{cm}^3 \text{s}^{-1})$	5.40×10^{-14}	3.03×10^{-14}	1.61×10^{-14}
$4\pi j_{H\beta}/n_e n_p (\text{erg cm}^3 \text{s}^{-1})$	2.21×10^{-25}	1.24×10^{-25}	6.58×10^{-26}

Balmer-line intensities relative to $H\beta$ $0.48627 \mu\text{m}$

$j_{H\alpha} 0.65646/j_{H\beta}$	3.03	2.86	2.74
$j_{H\beta} 0.48627/j_{H\beta}$	1.	1.	1.
$j_{H\gamma} 0.43418/j_{H\beta}$	0.459	0.469	0.475
$j_{H\delta} 0.41030/j_{H\beta}$	0.252	0.259	0.264
$j_{H\epsilon} 0.39713/j_{H\beta}$	0.154	0.159	0.163
$j_{H\delta} 0.38902/j_{H\beta}$	0.102	0.105	0.106
$j_{H\eta} 0.38365/j_{H\beta}$	0.0711	0.0732	0.0746
$j_{H\zeta} 0.37990/j_{H\beta}$	0.0517	0.0531	0.0540

-
- Radio-frequency - H β method
 - Nebulae with the strongest extinction cannot be observed in the optical wavelengths.
 - But, the radio-frequency continuum would be optically thin.
 - The line ratios depend on the ratio $n_+ \langle Z^2 \rangle / n_p$ where n_+ is the number density of all ions, because the free-free emission contains contributions from all ions.

$$\frac{n_+ \langle Z^2 \rangle}{n_p} \approx 1 + \frac{n(\text{He}^+)}{n_p} + 4 \frac{n(\text{He}^{++})}{n_p}$$

- The temperature dependence of $j_\nu / j_{\text{H}\beta}$ is approximately as $T^{1/3}$. This is considerably more rapid than an optical recombination-line ratio.

7.3 Dust within H II Regions

- Presence of Dust within H II regions
 - Many nebulae show “absorption” features that cut down the nebular emission and starlight from beyond the nebula.
 - Globules & Elephant-trunk:
 - ▶ Very dense small features of this kind are often called “globules.”
 - ▶ The features at the edges of nebulae are known as “elephant-trunk” or “comet-tail” structures.

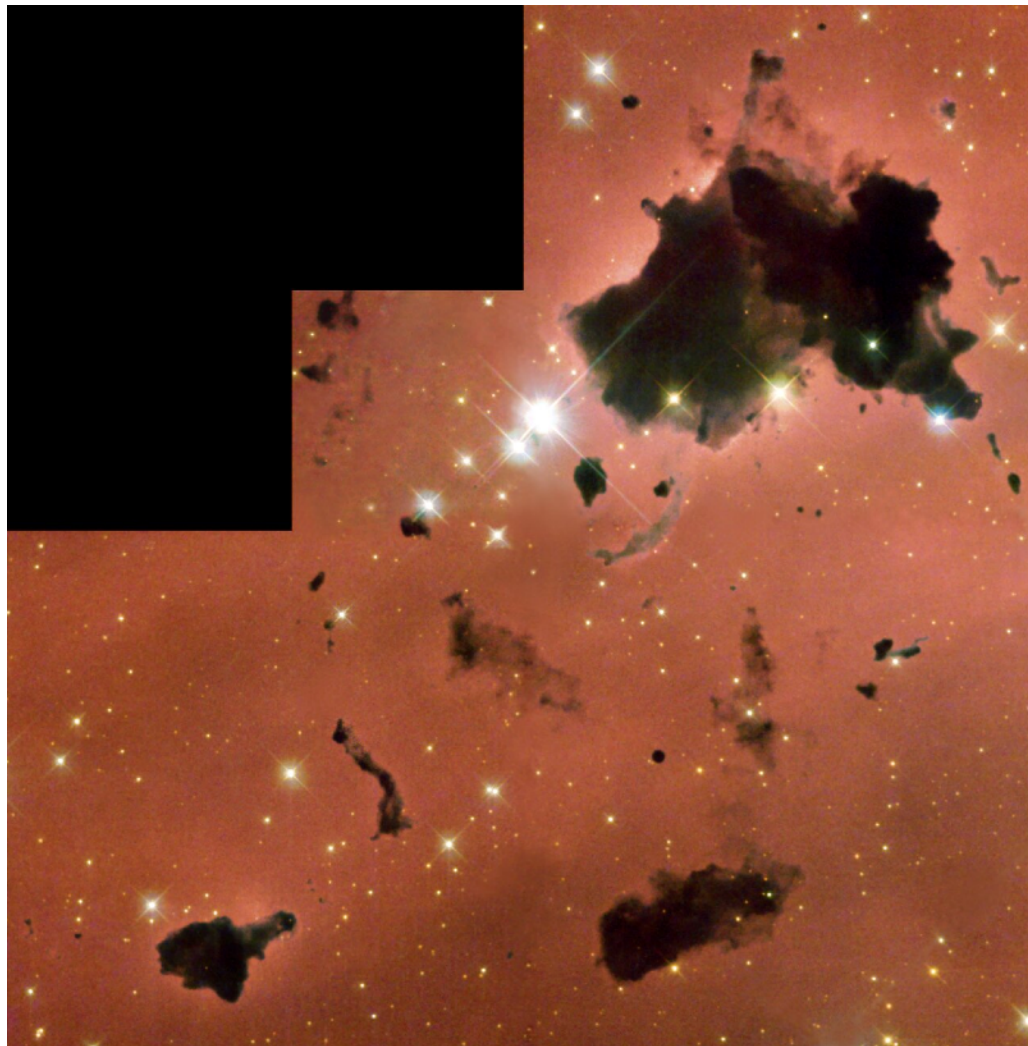


[Figure 7.2] Numerous globules in the H II region IC 2944
Credit: NASA/ESA and The Hubble Heritage Team (STScI/AURA)

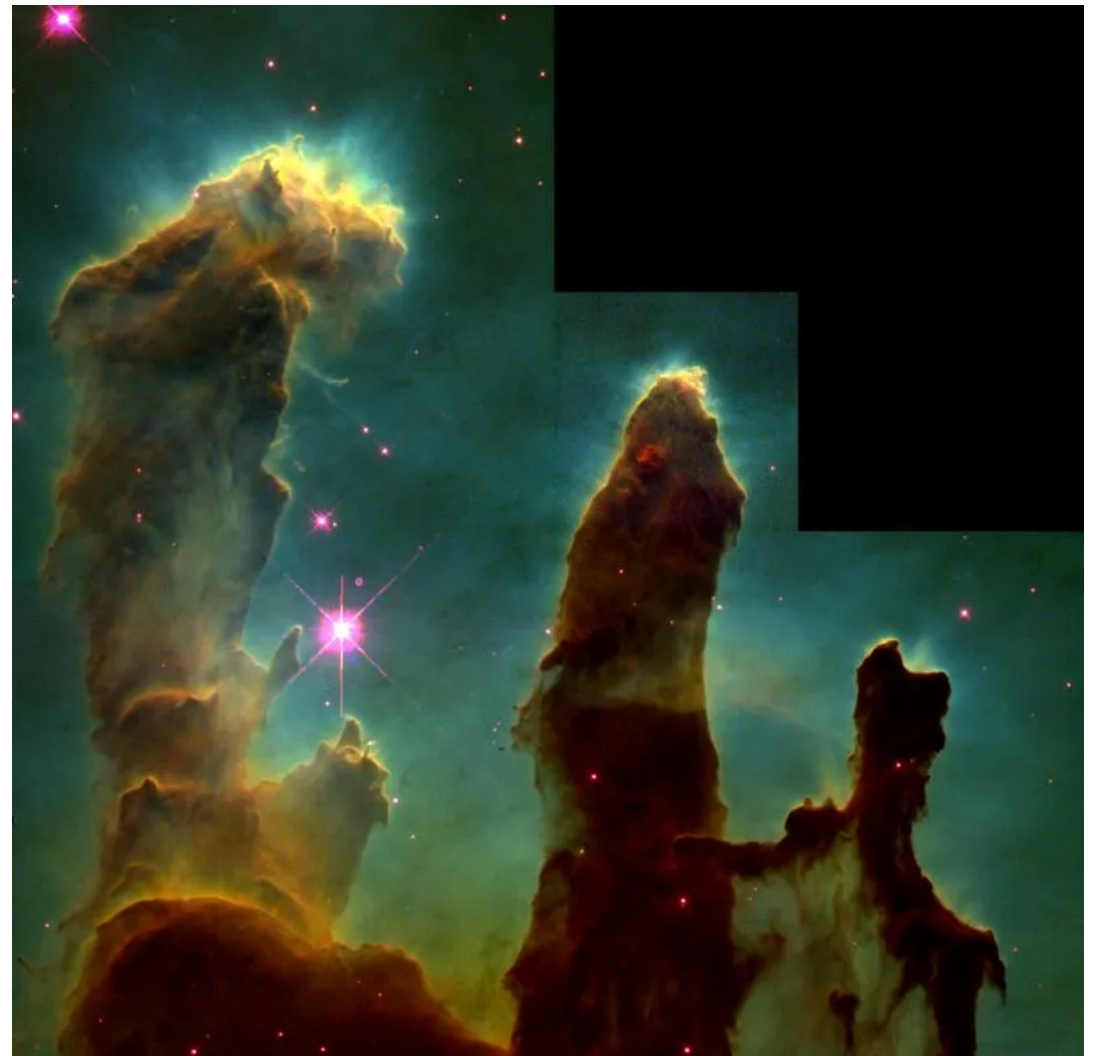


[Figure 7.3] The “Pillars of Creation”
Elephant-trunk structures in the H II region NGC 6611
Credit: NASA/ESA J. Hester and P. Scowen (STScI/AURA)

-
- IC 2944
 - ▶ Almost completely dark ones - they have a large optical depth (perhaps $\tau > 4$) and are on the near side of the nebula
 - ▶ A few large absorption features - they are not so close to the nebula.
 - Optical depth \Rightarrow the amount of dust
 - ▶ Measurements of optical depths can be used to estimate the amount of dust if its optical properties are known.
 - ▶ If, in addition, the gas-to-dust ratio is known, the total mass in the structure can be estimated.
 - Dust-scattered continuum
 - Dust particles scatter not only (1) the continuum radiation of the stars within nebulae but also (2) the nebular line + continuum emission. Therefore, low-resolution spectroscopic data, and narrow band filter maps would contain both the stellar + nebular components.
 - How to measure the “pure” dust-scattered continuum:
 - ▶ Measurements of this scattered continuum must be made with sufficient spectral resolution to avoid the strong nebular line emission.
 - ▶ The continuum maps may also be obtained using narrow band filters.
 - ▶ Measurements of an H II recombination line (e.g., $H\beta$) are required to calculate the expected nebular atomic continuum caused by bound-free and free-free emission. These contribution is subtracted from the observed continuum data, and the remainder represents the dust-scattered continuum.
 - The presence of the dust-scattered continuum is directly confirmed by the observations of the He II $\lambda 4686$ absorption line (e.g., in NGC 1976), which cannot arise in absorption in the nebular gas.

-
- Interpretation of observations
 - is not straightforward because of the complicated (and unknown) geometry.
 - The amount of scattered light depends upon these factors.
 - **The “single” dust scattering problem** in a spherical, homogeneous nebula illuminated by a single central star.
 - Assuming that the nebula is optically thin, the flux of starlight at a radius r from the star is

$$F_\lambda = \pi I_\lambda = \frac{L_\lambda}{4\pi r^2} \text{ where } L_\lambda = \text{luminosity of the star}$$

- Let's define
 - n_D = the number of dust particles per unit volume in the nebula
 - C_λ = the extinction cross section per a dust grain at the wavelength λ
 - $n_D C_\lambda$ = the extinction cross section per unit volume
 - a_λ = the albedo, the fraction of the radiation that is removed (i.e., scattered) from the flux
 - $1 - a_\lambda$ = the fraction that is absorbed
- Then, the emission coefficient (per unit volume per unit solid angle) due to scattering is

$$j_\lambda = \frac{1}{4\pi} a_\lambda \cdot n_D C_\lambda \cdot F_\lambda = \frac{a_\lambda n_D C_\lambda L_\lambda}{16\pi^2 r^2} \text{ at radius } r, \text{ if the scattering is spherically symmetric.}$$

- The intensity of the scattered continuum radiation is then

$$I_\lambda(b) = \int j_\lambda ds = \frac{a_\lambda n_D C_\lambda L_\lambda}{16\pi^2} \frac{2}{b} \cos^{-1}\left(\frac{b}{r_0}\right)$$

for a line of sight with an impact parameter b (the projected radius; the perpendicular distance between the line of sight and the central star) in a spherical nebula of radius r_0 .

- Now, compare this with the $H\beta$ surface brightness from the same nebula with a Stromgren radius r_1 ,

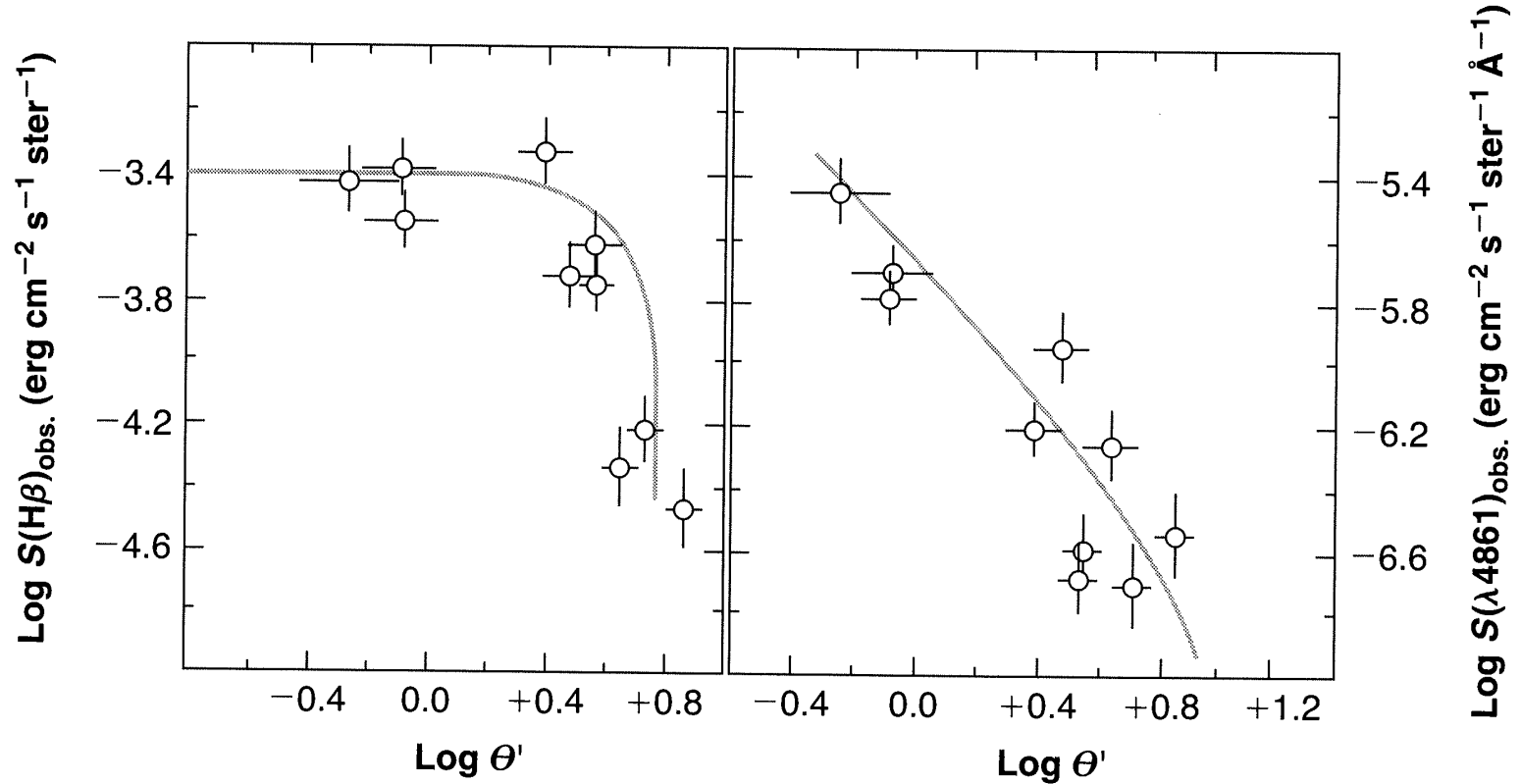
$$I_{H\beta}(b) = \int j_{H\beta} ds = \frac{1}{4\pi} n_p n_e \alpha_{H\beta}^{\text{eff}} 2 \sqrt{r_1^2 - b^2}$$

[Figure 7.5]

The two surface brightness distributions are compared with observational data of NGC 6514.

The nebular is the most nearly symmetric H II regions illuminated by a single dominant central star.

The model is a reasonable representation of this nebula.



- **Gas-to-dust ratios in H II regions**

- The ratio between the continuum and H β surface brightnesses is

$$\frac{I_{\text{H}\beta}(b)}{I_\lambda(b)} = \left[\frac{n_p n_e \alpha_{\text{H}\beta}^{\text{eff}} h \nu_{\text{H}\beta}}{a_\lambda n_D C_\lambda} \right] \left(\frac{4\pi D^2}{L_\lambda} \right) \left(\frac{r_0 r_1}{D^2} \right) \left[\frac{(b/r_0) \sqrt{1 - (b/r_1)^2}}{\cos^{-1}(b/r_0)} \right]$$

where D = the distance of the nebula from the observer.

- ▶ The first factor in square brackets involves atomic properties and dust properties.
- ▶ The second factor is the reciprocal of the stellar flux observed at the earth.
- ▶ The third factor is the product of the angular radii (r_0/D of the continuum and r_1/D of H β).
- ▶ The fourth factor gives the angular dependence of the surface brightnesses, expressed in dimensionless ratios.
- Therefore, the first factor can be determined from the measurements of (1) the surface brightness profiles and (2) the flux from the star.
- Next, n_e can be determined either (1) from the H β surface brightness itself or (2) from the [O III] or [S II] line ratios.
- Finally, $n_p/a_\lambda n_D C_\lambda$, proportional to the gas-to-dust density ratio can be determined.

-
- The ratios found in this way from continuum observations of H II regions:

[Table 7.3] Gas-to-dust ratios in H II regions

Nebula	Assumed n_e (cm $^{-3}$)	$n_p/a_\lambda n_D C_{\lambda 4861}$ (cm $^{-2}$)
NGC 1976 (inner)	model	1.4×10^{22}
NGC 1976 (outer)	model	5×10^{20}
NGC 6514	130	4×10^{20}
NGC 6523	44	2×10^{21}
NGC 6611	55	2×10^{21}
Field	—	2×10^{21}

- Typical densities of globules

Suppose an opaque globule with radius of 0.05 pc and an optical depth $\tau_{H\beta} \geq 4$.

Assuming that the dust in the globule has the same properties as that in the ionized part, $n_D \geq 2 \times 10^{-8} \text{ cm}^{-3}$.

Further supposing that the gas-to-dust ratio is the same, we find that $n_H \geq 2 \times 10^4 \text{ cm}^{-3}$.

-
- Scattering of Emission Lines
 - Observations show that much of the line radiation observed in the faint outer parts of NGC 1976 actually consists of scattered photons that were originally emitted in the bright central parts of the nebula.
 - If the albedo were $a_\lambda = 1$ at all wavelengths, the scattering would not affect the total emission-line flux from the whole nebula, because no photons will be absorbed, although the scattering would transfer the apparent source of photons.
 - In reality, $a_\lambda < 1$ and a fraction of emission line photons is destroyed by dust within the nebula.
 - Therefore, the procedure for correcting observed line intensities for interstellar extinction described in Section 7.2 is only approximately correct, because it is based on stellar measurements, in which radiation scattered by dust along the line of sight does not reach the observer.
 - However, numerical models show that the correction procedure is approximately correct and give very nearly the right relative emission line strengths. This is because the wavelength dependence of the extinction is relatively smooth and the wavelength differences between the usually observed lines are not significantly different.
 - Naturally, the longer the range of wavelengths over which these corrections are applied, the larger the error may be.

7.4 Infrared Thermal Emission

- Dust is also observed in H II regions by its IR thermal emission.
 - The measured nebular IR continuous radiation is approximately 10^2 to 10^3 times larger than the free-free and bound-free continua, and can only arise by radiation from dust.
 - Dust is heated by the absorption of UV and optical radiation from the stars.
- Dust emits a **dilute blackbody spectrum (modified blackbody)**.
 - Therefore, measurements at two wavelengths approximately determine its temperature.
 - For instance, the measured intensity of the Ney-Allen nebula at $11.6 \mu\text{m}$ is about $10^{-3}B_\nu(T_c)$. This indicates that it has an effective optical depth of about $\tau_{11.6\mu\text{m}} \approx 10^{-3}$.
 - [Note] Kirchhoff's law: $j_\nu = \kappa_\nu B_\nu \Rightarrow I_\nu = j_\nu \Delta s = \kappa_\nu \Delta s B_\nu = \tau_\nu B_\nu$ (if $T = \text{constant}$)
- Broad and narrow IR features
 - silicates - a relatively sharp peak at $\lambda \approx 9.8 \mu\text{m}$ with the FWHM of $\sim 2.5 \mu\text{m}$
 - PAHs (polycyclic aromatic hydrocarbon molecules) - relatively narrower features at $\lambda 3.28, 3.4, 6.2, 7.7, 8.6$, and $11.3 \mu\text{m}$: These are too broad to be emission lines of ions, and are most probably the result of IR fluorescence from vibrationally excited, PAHs, consisting of many atoms, such as $\text{C}_{24}\text{H}_{12}$, or more generally, hydrogenated amorphous carbon particles.
 - PAHs are excited by UV and optical radiation, and then decay to excited vibrational levels which emit photons in the $3.28 \mu\text{m}$ and other bands as they decay to the ground level.
 - Quantum heating: The resulting emission is not at any equilibrium temperature, but rather is due to the temperature spike that immediately follows absorption of the photon, and the subsequent cooling that continues until the arrival of the next photon. This “quantum heating” is important for small particle with small heat capacity, whose temperature is affected by a single photon.

- The measured IR flux at $\lambda \approx 400 \mu\text{m}$ is roughly proportional to the measured radio-frequency flux.
 - The radio-frequency flux from a nebula is proportional to the number of recombinations.
 - Thus, the IR flux is also proportional to the number of recombinations, or equivalently to the number of ionizations, or the number of ionizing photons absorbed in the nebula.
 - Is this correlation mainly caused by Ly α absorption? No!
 - Every ionization (in an optically thick nebula) leads ultimately to a recombination and the emission of an Ly α or of two photons ($2^2S \rightarrow 1^2S$).
 - Since the Ly α photons are scattered many times by resonance scattering before they escape, every Ly α photon would be absorbed by dust in the nebula and its energy is re-emitted as IR radiation.
 - If this is the case, then the IR-to-radio-frequency flux ratio would be

$$\frac{j_{\text{IR}}}{j_\nu} = \frac{n_p n_e (\alpha_B - \alpha_{2^2S}^{\text{eff}}) h\nu_{\text{Ly}\alpha}}{4\pi j_\nu} \quad \text{where}$$

$$j_\nu(\text{HI}) = \frac{1}{4\pi} n_p n_e \gamma_\nu(\text{H}^0, T) \quad (\text{see Chapter 4})$$

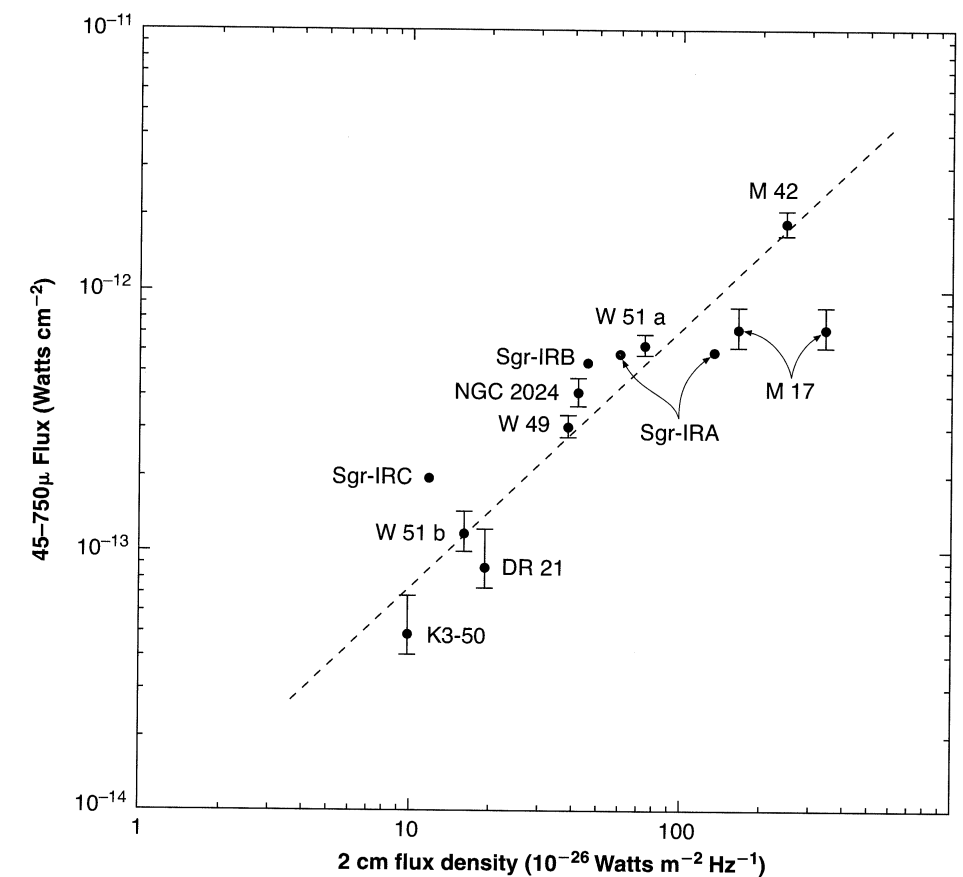


[Figure 7.7]
FIR (45-170 μm) flux vs. radio-frequency flux for several H II regions.

This ratio depends on temperature very weakly, and j_{IR} and j_{ν} have the same density dependence.

Predicted ratio is $j_{\text{IR}}/j_{\nu} = 1.3 \times 10^{15} \text{ Hz}$ for $\nu = 1.54 \times 10^{10} \text{ Hz}$ and $T = 7500 \text{ K}$. However, the observed ratio was $j_{\text{IR}}/j_{\nu} = 7.5 \times 10^{15} \text{ Hz}$, five times higher than the predicted.

- ▶ Conclusion: the IR emission cannot be accounted for by absorption of Ly α alone.
- **The IR radiation is predominantly caused by absorption of the stellar continuum radiation with $\nu < \nu_0$** , in addition to Ly α (some of LyC radiation is also absorbed by the dust).

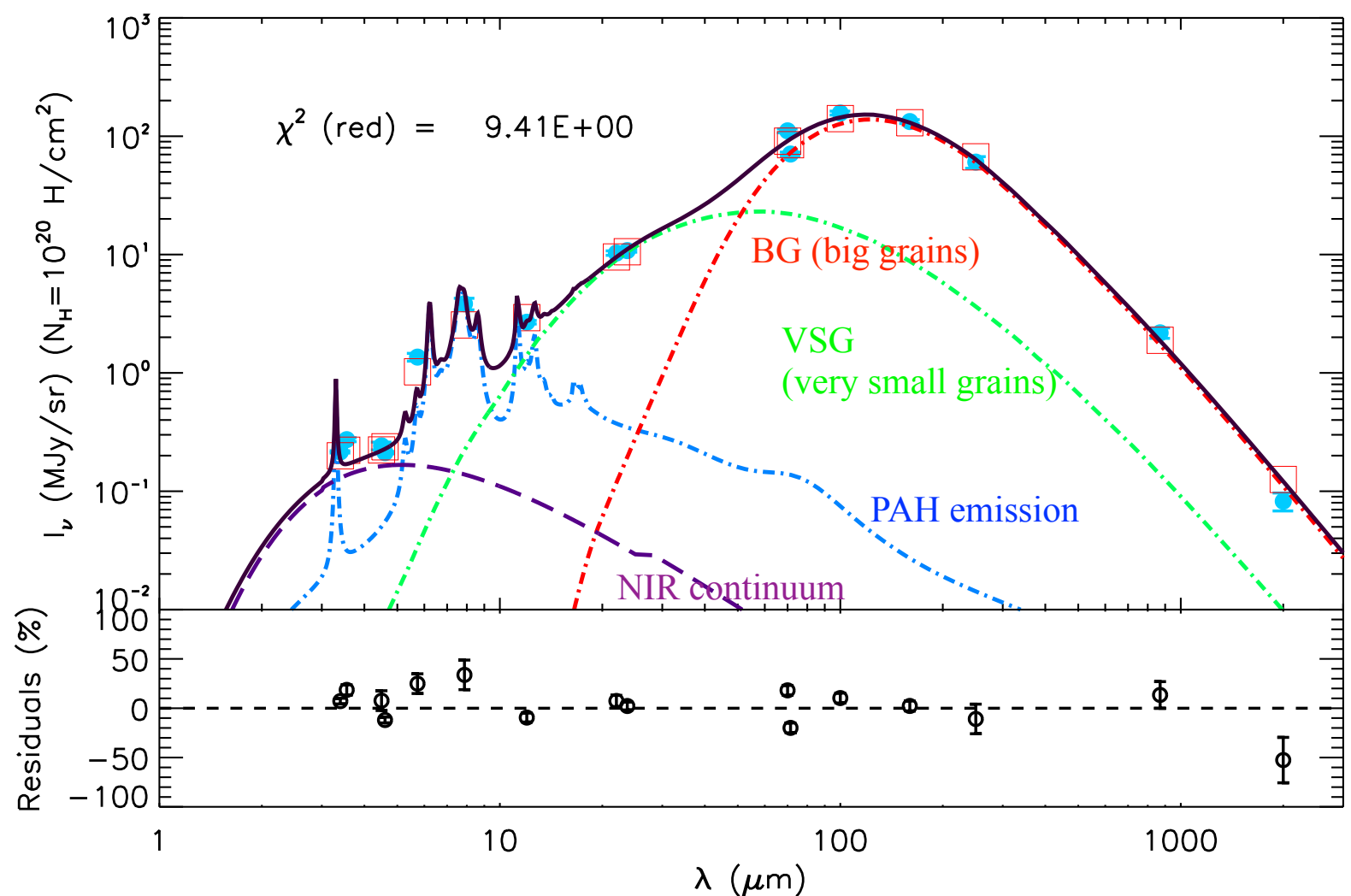
An example of SED models for H II regions in M33

The NIR continuum is modelled using a black body with a temperature of 1000 K.

The origin of this NIR continuum is uncertain.

In a sample of 45 normal star-forming galaxies, reflection nebulae, and the diffuse cirrus emission in the Milky Way, this component has been observed.

Relaño et al. (2016, A&A, 595, A43)



-
- Dust in PNs
 - There was little earlier evidence of dust in PNe before the IR observations were made.
 - The IR measurements revealed that the continuum in $5 - 18 \mu\text{m}$ is 10 to 100 times stronger than the extrapolated free-free and bound-free continua.
 - Observations in IR (out to $100 \mu\text{m}$) show that the IR continua of most PNe peak at $\sim 30 \mu\text{m}$, suggesting $T_D \sim 100 \text{ K}$.

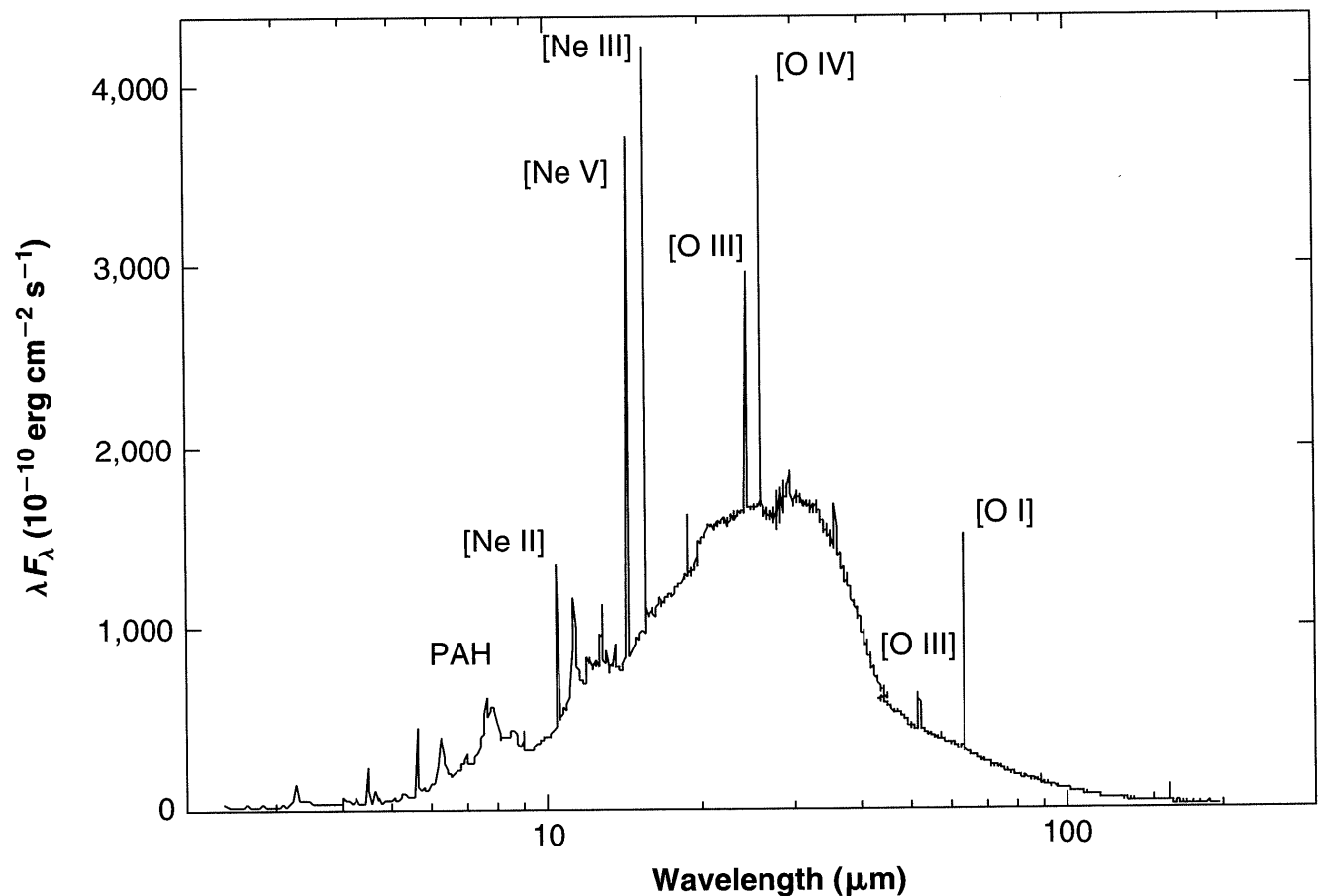


[Figure 7.8] The observed IR spectrum of the PN NGC 7027. The continuum is largely due to dust emission.

7.5 Formation and Destruction of Dust Particles

- In H II regions, the optical properties of dust grains, and the dust-to-gas ratio are approximately the same as in the general ISM. Three questions arise:
 - How are the dust particles initially formed?
 - How long do they survive?
 - How are they ultimately destroyed?
- Formation of dust particles
 - They cannot initially form by atomic collisions at even the highest densities in gaseous nebulae, although they, once formed, can grow by accretion of individual atoms from the interstellar gas and by low energy grain-grain collisions.
 - In PNe, gaseous shells ejected by their central stars, the dust must have been present in the atmosphere of the star or must have formed during the earliest stages of the process, at the high densities that occurs close to the star.
 - IR observations show that many cool giants and supergiant stars have dust shells around them.
 - The outer layers of cool stars can be cool, dense, and predominantly molecular. H_2 and CO are the most abundant molecules. (they are most abundant and have large dissociation energies).
 - **[Silicate]** If the abundance of O is greater than C in the outer layers of the star (as in the solar system), then most C will go into CO. The remaining O eventually form the silicate grains.
 - **[Graphite]** Graphite is formed by similar processes but in regions where the abundance of C is greater than O.

- Destroy of Grains

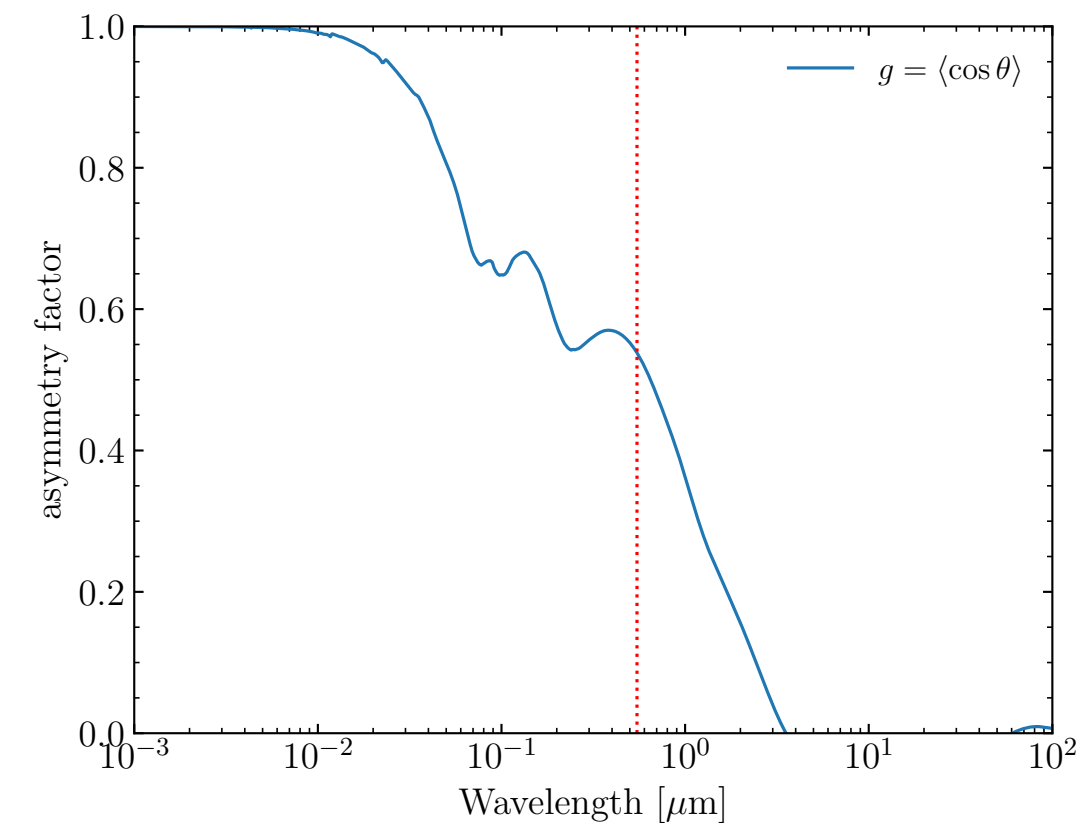
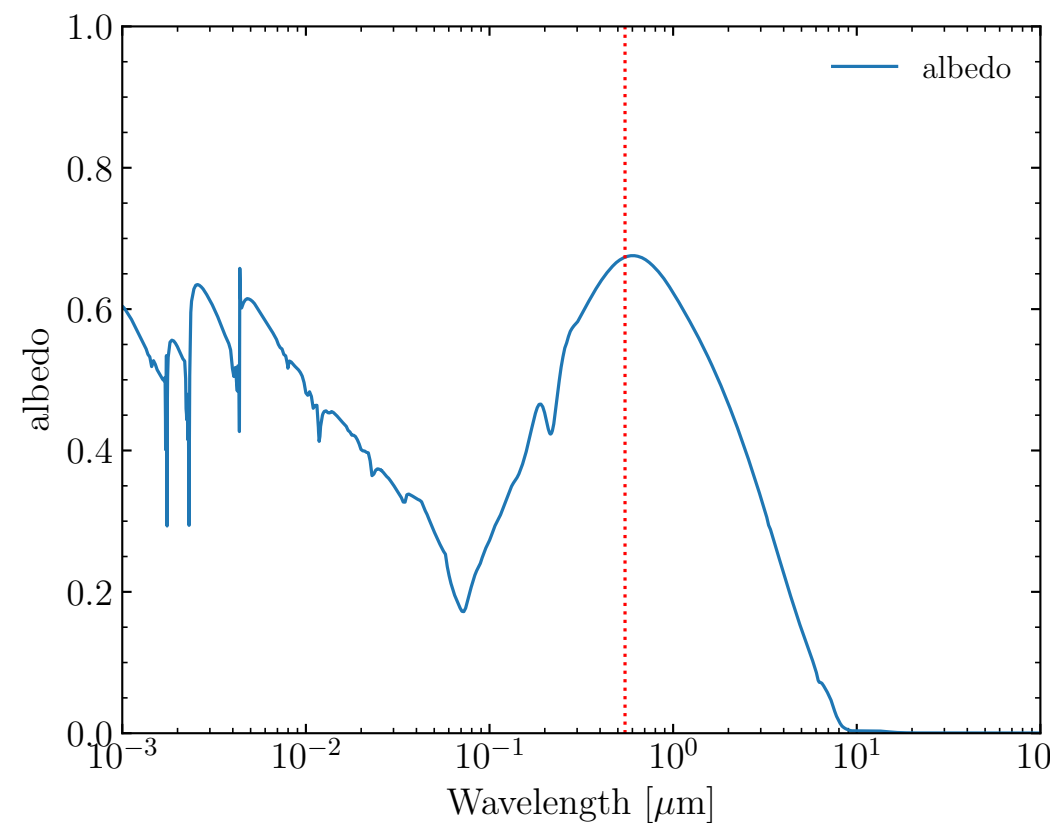
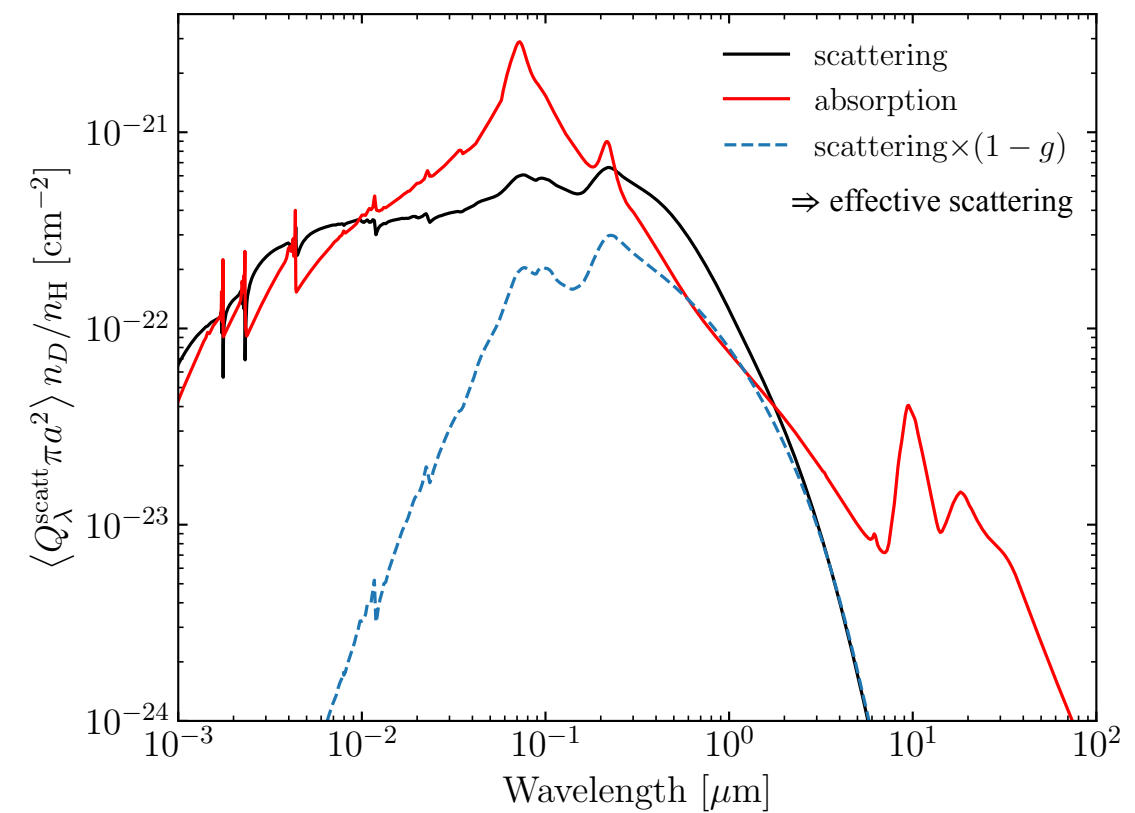
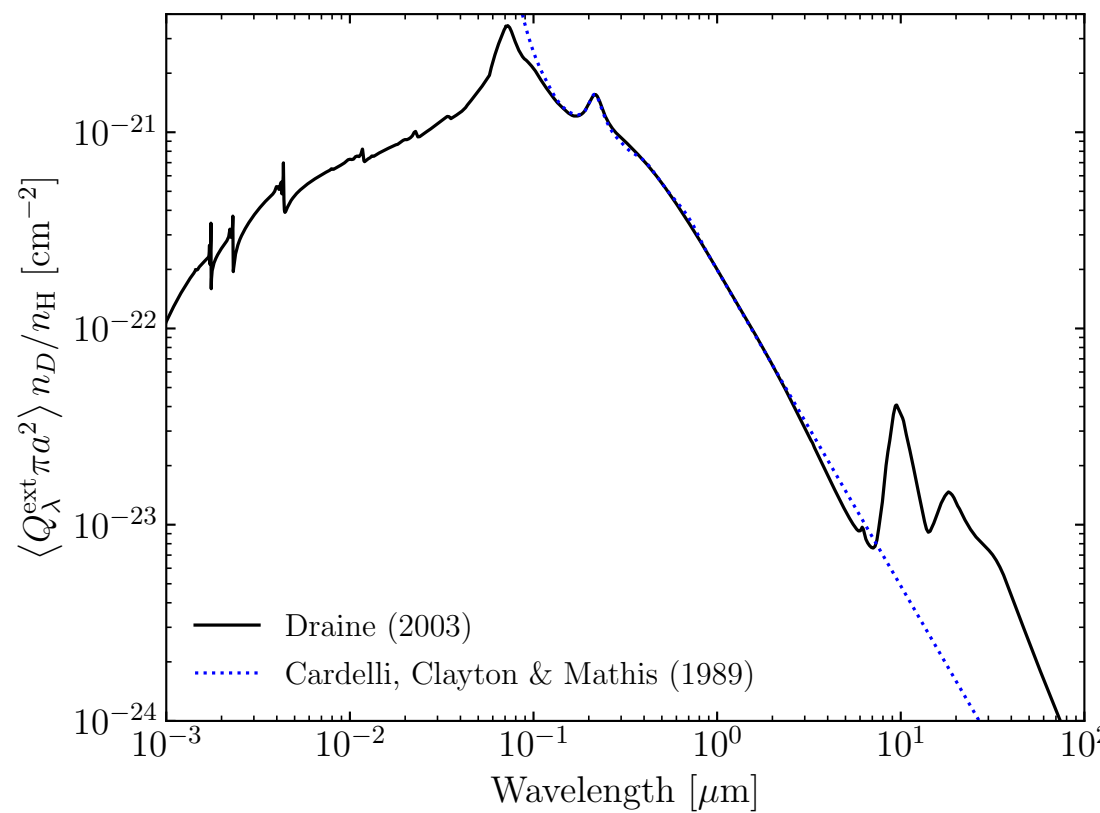
reference: Jones (2004, *Astrophysics of Dust*, ASP Conference Series 309)

- Dust particles in a nebula are immersed in a harsh environment containing both ionized gas and high-energy photons.
- **Sputtering** is the process in which **collisions of ions with a dust particle** knock atoms or molecules out of its surface. This is important if the gas is quite hot, but is inefficient at nebular temperature.
- **Photodesorption by grain charging effects:** High-energy photons can be absorbed and cause the ejection of photoelectrons. If this process is efficient enough the coulomb forces due to the positive charge can exceed the binding energy (tensile strength) of the grain, leading to its disruption.
- **Sublimation:** If a grain becomes hot enough (50-100 K for ices, and $T_{\text{grain}} > 1,000$ K for graphite or silicate), outer layers will evaporate and the grain is destroyed by sublimation.
- However, elements like Al and Ca, which are mostly found within dust grains in the ISM, are also strongly depleted from the gas phase in nebulae, suggesting these processes do not destroy a significant fraction of the grains.
- **Dust size distribution:** A variety of processes (grain-grain collisions and sputtering, etc) occurring near the shock front cause larger grains to be fragmented into smaller ones with ranges of sizes. This process probably establishes the observed distribution of sizes.
- The observed variation in the ratio of total to selective extinction is partly due to different regions having different histories of shock passage and so a different ratio of a small to large grains.

7.6 Grain Opacities

- Mie scattering theory
 - A theoretical extinction curve that may match observation is derived from “the index of refraction of materials + grain shapes (usually spherical) + a size distribution (number of grains as a function of their sizes).”
- Definitions
 - Extinction coefficient : $\kappa_\lambda(a) = n_D C_\lambda = Q_\lambda(a) \pi a^2 n_D$.
 a = the size of a grain, n_D = number density of dust grains
 $\pi a^2 n_D$ = the geometrical cross section (projected grain area) per unit volume.
 - $Q_\lambda(a)$ = the effective cross section (dimensionless quantity)
 $Q_\lambda(a) \approx 1$ for $a \gg \lambda$: the grain is much larger than the wavelength of light
 $Q_\lambda(a) \propto \lambda^{-\beta}$ for $a \ll \lambda$, where $\beta = 1 - 2$ depending on the composition of the grain.
 - $\langle \pi a^2 Q_\lambda n_D \rangle$ = the cross section per dust grain at a wavelength λ , averaged over the grain size distribution.
- Extinction = Absorption + Scattering
 - Absorption : the photon’s energy is absorbed by the grain and converted into internal heat.
 - Scattering : a photon is merely deflected (scattered) from its path.
 - Stellar extinction observations measure the sum of absorption and scattering.

- Theoretical and Empirical Extinction Curves.



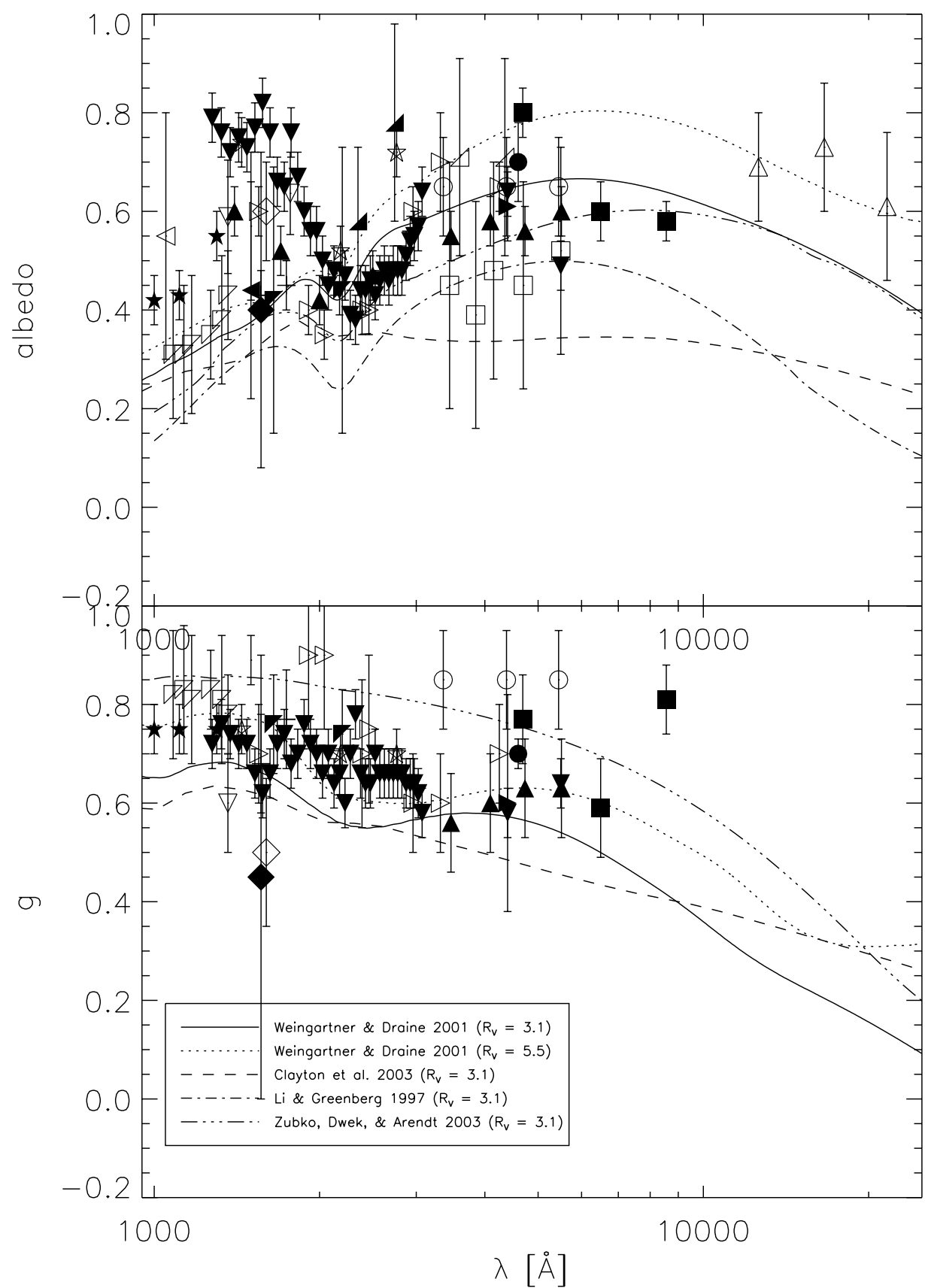
- Properties of Absorption
 - The absorption curve peaks near the ionization threshold of hydrogen.
 - Grains are more likely to absorb ionizing radiation than hydrogen when the neutral fraction of hydrogen is less than $n(\text{H}^0)/n(\text{H}) \lesssim 3 \times 10^{-4}$.

Note that $\sigma_{\text{pi}}(\nu) \approx \sigma_0 (h\nu/I_{\text{H}})^{-3}$ for $I_{\text{H}} \lesssim h\nu \lesssim 100I_{\text{H}}$ where $\sigma_0 = 6.304 \times 10^{-18} \text{ cm}^{-2}$
 - The broad absorption features are believed to be due to the PAHs ($\lambda \sim 2175 \text{\AA}$) and silicate ($\lambda \sim 9.7, 18 \mu\text{m}$) components.
 - At very high energies the absorption is simply the total photoelectric opacity of the atoms within the grain.
- Properties of Scattering
 - Calculations of the ionization structure of model nebulae usually discount (subtract) forward scattering, in which the path of a photon is only slightly altered.
 - The grain asymmetry factor g accounts for this fraction.
 - The $\langle \pi a^2 Q_{\text{scatt},\lambda} (1 - g) n_D \rangle$ discounts the forward scattering.
 - Grains have a small albedo (are strongly absorbing) at long wavelengths (IR).
 - The albedo is roughly 0.5 through the UV and optical.
 - At ionizing energies, the grains are strongly absorbing when forward scattering is discounted.

- Comparison with Observations

Karl D. Gordon (2004)
 Astrophysics of Dust
 (ASP Conference Series, Vol. 309, 77)

https://www.stsci.edu/~kgordon/Dust/Scat_Param/scat_data.html



7.7 Effects of Grains on Surrounding Gas

- Grains seem to be about as important as He in their effects on the ionization and temperature structure of a nebula.
 - Grains absorb some of the ionizing continuum and their photoionization can heat the gas.
- Electric Charge of a dust grain in a nebula
 - The charge results from the competition between (1) photoejection of electrons from the solid particle by the UV photons, which tends to make the charge positive, and (2) captures of positive ions and electrons from the nebular gas, which tend to make the charge more positive and negative, respectively.
 - Typical grain materials have work functions (ionization potential) between 4 and 10 eV.
- Equilibrium equation for the charge on a grain

Photoelectric Emission:

- The rate of increase of the charge Ze due to photoejection of electrons can be written

$$\left(\frac{dZ}{dt} \right)_{pe} = \pi a^2 \int_{\nu_K}^{\infty} \frac{4\pi J_{\nu}}{h\nu} Q_{\nu}^{\text{abs}} \phi_{\nu} d\nu$$

where ϕ_{ν} is the photodetachment probability ($0 \leq \phi_{\nu} \leq 1$) for a photon that strikes the geometrical cross section of the particle.

- **[Threshold]** If the dust particle is electrically neutral or has a negative charge, the effective threshold is $h\nu_K = h\nu_c$ (the threshold of the material). If the particle is positively charged, the lowest energy photoelectrons cannot escape. Therefore, the threshold is

$$\begin{aligned} h\nu_K &= h\nu_c + Ze^2/a & Z < 0 \\ &= h\nu_c & Z \leq 0 \end{aligned}$$

Here, $-Ze^2/a$ = the potential energy at the surface of the particle.

Collisional Charging:

- The rate of increases of the charge due to capture of electrons is

$$\left(\frac{dZ}{dt} \right)_{ce} = -\pi a^2 n_e \sqrt{\frac{8kT}{\pi m_e}} \xi_e Y_e$$

$$\langle v \rangle = \int_0^\infty v f(v) dv = \sqrt{\frac{8kT}{\pi m_e}} = \text{mean speed for the Maxwell distribution of speed.}$$

ξ_e = the electron-sticking probability ($0 < \xi_e < 1$)

$$Y_e = \begin{cases} 1 + \frac{Ze^2}{a} \frac{1}{kT} & Z > 0 \\ \exp(Ze^2/akT) & Z \leq 0 \end{cases}$$

Y_e is the factor due to the attraction or repulsion (Coulomb focusing) of the charge on the particle.

- The rate of increases of the charge caused by capture of protons is

$$\left(\frac{dZ}{dt} \right)_{cp} = \pi a^2 n_p \sqrt{\frac{8kT}{\pi m_H}} \xi_p Y_p$$

$$Y_p = \begin{cases} 1 - \frac{Ze^2}{a} \frac{1}{kT} & Z \leq 0 \\ \exp(-Ze^2/akT) & Z > 0 \end{cases}$$

See Chap. 25 in "Physics of the Interstellar and Intergalactic Medium" (Draine) for the derivation of the formulae

Chap 4 in "The Physics of the Interstellar Medium" (Dyson and Williams)

Equilibrium Equation

- Thus, the charge on a particle can be found from the solution of the equation:

$$\frac{dZ}{dt} = \left(\frac{dZ}{dt} \right)_{\text{pe}} + \left(\frac{dZ}{dt} \right)_{\text{ce}} + \left(\frac{dZ}{dt} \right)_{\text{cp}} = 0$$

In this equation, the factor πa^2 cancels out, but the dependence on a through the surface potential remains.

The equation can be solved numerically for a model nebula for which the density and the radiation field are known.

- [General result] In the inner part of an ionized nebula, photoejection dominates and the particles are positively charged. In the outer parts, where the UV flux is smaller, the collision with electrons dominate and the particles are negatively charged because more electrons strike the particle.
- Grain Temperature

Heating is caused by absorption of the local radiation field and collisions with gas

- The radiation field is usually most important and the heating rate is given by

$$\dot{E}_{\text{heat}} = \pi a^2 \int_0^\infty \frac{4\pi J_\nu}{h\nu} Q_\nu^{\text{abs}} (1 - \phi_\nu) d\nu \quad \text{for the radiation field } J_\nu \text{ incident upon dust grains.}$$

For $\nu < \nu_K$, $\phi_\nu = 0$ (all the energy of absorbed photons heat the grain). For $\nu > \nu_K$, $\phi_\nu \neq 0$ (some of the energy goes into the photoelectron, with much goes into heating the grain)

Cooling is predominantly due to emission in the IR continuum.

- The cooling rate is given by Kirchhoff's law.

The cooling due to a spherical grain of radius a is

$$\dot{E}_{\text{cool}} = n_{\text{D}}(\pi a^2) \int_0^{\infty} Q_{\nu}^{\text{abs}} 4\pi B_{\nu}(T_{\text{D}}) d\nu \quad \text{where } T_{\text{D}} \text{ is the dust temperature.}$$

The cooling mainly occurs in the IR, where $\lambda \gg a$ and $Q_{\lambda}^{\text{abs}} \propto \lambda^{-1}$. As a result,

$$T_{\text{D}} \propto \left(\frac{L}{4\pi r^2 a} \right)^{1/5}$$

- For a representative particle with $a = 3.0 \times 10^{-5}$ cm, the dust temperature is $T_{\text{D}} \approx 100$ K at $r = 3$ pc from the star (with the 40,000 K blackbody radiation).

- In H II regions,
 - The ionization region is smaller than the dust-free case due to dust absorption of the LyC.

Near the central star

- The ionizing radiation field creates a positive charge, which then creates the attractive Coulomb force.
- The grain “ionization potential” is this Coulomb potential + the work function.
- Grain photoionization accounts for $\sim 30\%$ of the total heating in these regions.
- Smaller grains tend to have a larger potential and to be hotter, due to their smaller radius.
- Graphite is more highly charged than the silicates due to the larger cross section at higher energies.

In outer regions

- The radiation field is extinguished and grains recombine more rapidly than they are ionized, creating a negative charge

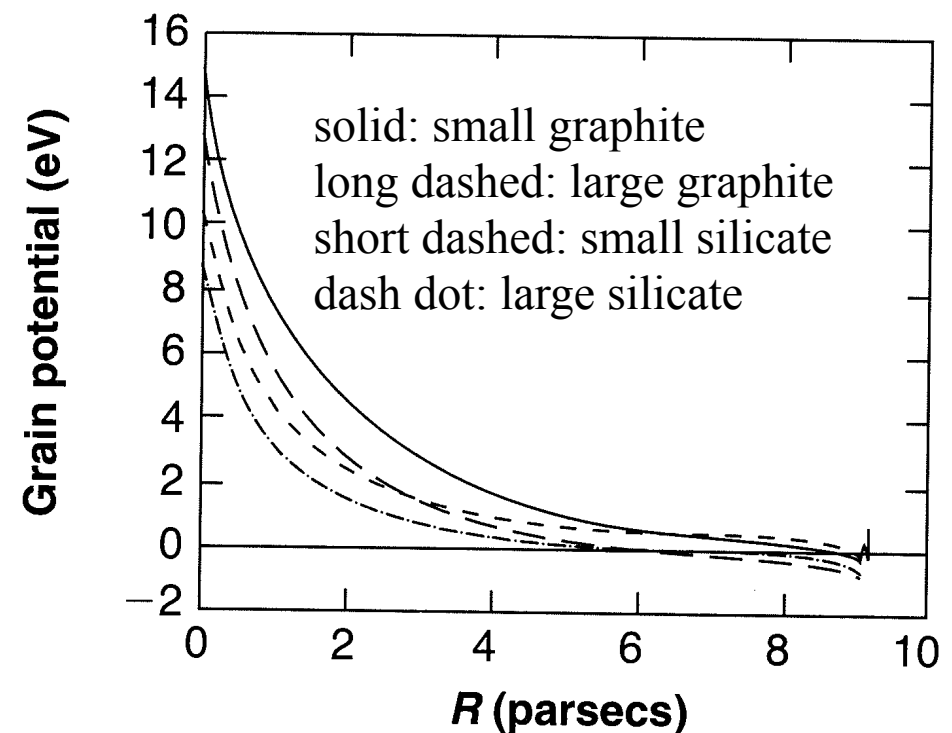


[Figure 7.10]

A 40,000 K black body source is assumed.
Here, small = $0.03 \mu\text{m}$, large = $0.2 \mu\text{m}$.

- Grain temperature

- The temperature is not strongly affected by the grain composition but the grain size is important.
- Small grains are hotter than large grains because Q^{abs} is smaller and they cool less efficiently in the IR.
- The total emission originating from large grains can be approximated by a single equilibrium temperature. However, it is not the case for small grains.
- Grains are hotter near the star.
- The total emission is the volume integral of the cooling rate and is strongly weighted to warmer regions due to the temperature dependence of the Planck function.

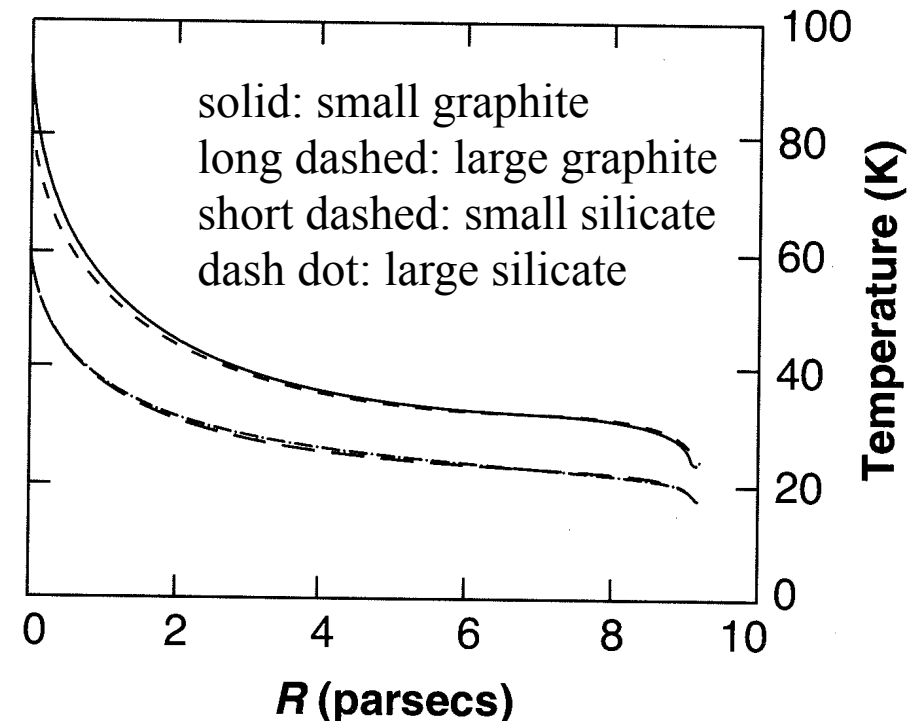


[Figure 7.10]
A 40,000 K black body source is assumed.
Here, small = 0.03 μm , large = 0.2 μm .

-
- Sublimation Temperature of ices
 - $T_{\text{sub}} = 20 \text{ K}$ for CH_4 (methane), $T_{\text{sub}} \approx 60 \text{ K}$ for NH_3 (ammonia), $T_{\text{sub}} \approx 100 \text{ K}$ for H_2O (water).
 CH_4 cannot be held anywhere in the nebula.
 NH_3 vaporizes except in the outer parts.
 H_2O evaporates only in the innermost parts.
 - $T_{\text{sub}} \approx 10^3 \text{ K}$ for graphite, silicate, and silicon carbide particles
Hence, they are less sublimated.
 - Polarization
 - Most of studies assume that grains are spherical, for simplicity. However, scattered light by grains and transmitted light through grains is found to be polarized.
 - This indicates that grains are (1) not non-spherical and (2) aligned with the galactic magnetic field ($B \sim 5 \mu\text{G}$).
 - Grains are thought to be composed of paramagnetic materials, interacting with magnetic fields. (1) Gas-grain collisions and the recoil caused by emitted or absorbed photons and (2) the radiative torque cause the grain to spin.
 - An interaction between the galactic magnetic field and the spinning grain help align it with the field.
 - Observations of polarization can give information on the geometry and strength of the galactic magnetic field.

7.8 Dynamical Effects of Dust in Nebulae

- Radiation Force
 - Dust particles in a nebula are subjected to radiation pressure from the central star.
 - However, the coupling between the dust and gas is very strong, so the dust particles do not move through the gas to any appreciable extent, but rather transmit the central repulsive force of radiation pressure to the entire nebula.

Radiation force on a dust particle of radius a by the central star is

$$F_{\text{rad}} = \pi a^2 \int_0^\infty \frac{F_\nu}{c} Q_\nu d\nu = \pi a^2 \int_0^\infty \frac{L_\nu}{4\pi r^2 c} Q_\nu d\nu, \text{ where } Q_\nu = Q_\nu^{\text{abs}} + Q_\nu^{\text{scatt}}(1 - g).$$

Most of the radiation from hot stars has $\lambda \ll a$. Then, $Q_\nu \approx 1$. In this case, $F_{\text{rad}} \approx \frac{a^2 L}{4r^2 c}$.

However, this is not true for very small particles or for very cool stars.

- The diffuse radiation field is more isotropic and its effect can be neglected in the radiation force.

Drag force: The force tends to accelerate the particle, but its velocity is limited by the drag on the particle due to its interaction with the gas.

- If the particle is neutral, this drag results from direct collisions of the ions with the grain, and the resulting force is

$$F_{\text{coll}} = \frac{4}{3} n_p \pi a^2 \left(\frac{8kT m_H}{\pi} \right) w \quad \langle v \rangle = \int_0^\infty v f(v) dv = \sqrt{\frac{8kT}{\pi m_e}}$$

where w is the velocity of the particle relative to the gas, assumed to be smaller than the mean thermal velocity.

Thus, the particle is accelerated until two forces are balanced, and reaches a terminal velocity

$$F_{\text{rad}} = F_{\text{coll}} \Rightarrow w_t = \frac{3L}{16\pi r^2 c n_p} \left(\frac{\pi}{8kTm_H} \right)^{1/2}, \text{ which is independent of the particle size.}$$

For instance, for a particle at a distance of 3.3 pc from an O star, $w_t = 10 \text{ km s}^{-1}$. The time required for a travel of 1 pc is about 10^5 yr .

- For charged particles, the Coulomb force increases the interaction between the positive ions and the particle significantly, and the drag on a charged particle has an additional term,

$$F_{\text{Coul}} \approx \frac{2n_p Z^2 m_H}{T^{3/2}} w$$

Comparison of F_{coll} with F_{Coul} shows that Coulomb effects dominate if $|Z| \geq 50$. In most regions of the nebula, the particles have a charge greater than this, the terminal velocity is even smaller and the particle motion relative to the gas is smaller yet.

Typical values are under 1 km s^{-1} . Under these conditions the dust particles are essentially frozen to the gas.

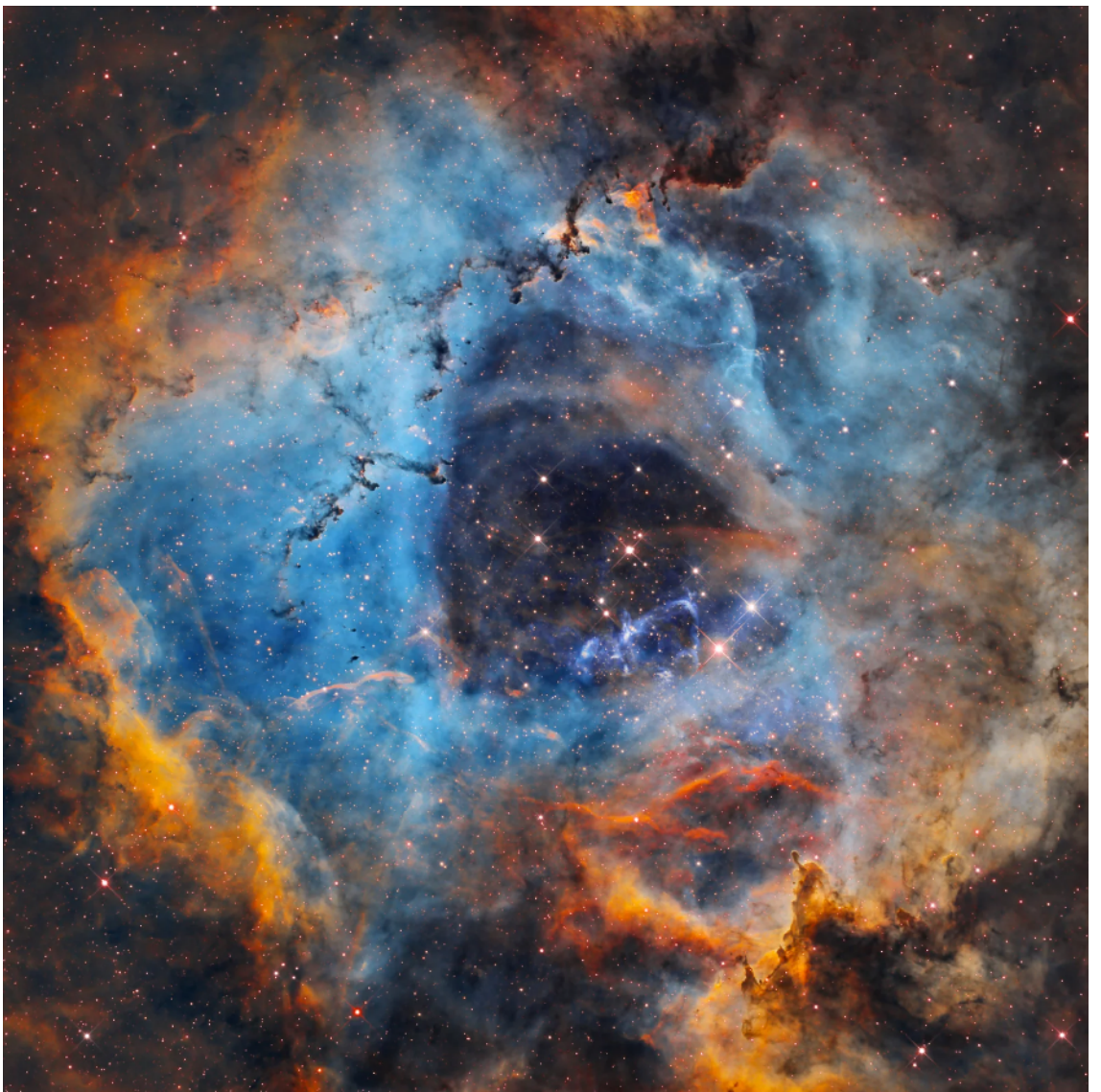
- Therefore, the radiation pressure on the particles acts on the nebular material, and the equation of motion of fluid contains this extra term:

$$\rho \frac{Du}{dt} = -\nabla P - \rho \nabla \phi + n_D \frac{a^2 L}{4r^2 c} \mathbf{e}_r \text{ where } \mathbf{e}_r \text{ is the unit vector in the radial direction.}$$

This acceleration can be appreciable, and the radiation-pressure effects should be taken into account in a model of an evolving H II region.

- Calculations showed that old nebulae will tend to develop a central “hole” that has been swept clear of gas by the radiation pressure upon the dust.

An example of a real nebula is NGC 2244.



credit: Shawn Nielsen, VisibleDark

- Concluding Remarks

- Observations clearly show that dust exist in nebulae, but its optical and physical properties are still not accurately known.
- Models and calculations carried out to date must be considered schematic and indicative rather than definitive.